

DENSITY DEPENDENCE OF TRANSPORT IN SLIT MICROPORES

Owen G. Jepps¹, Suresh K. Bhatia¹, Debra J. Searles²

¹ *Division of Chemical Engineering, University of Queensland, Brisbane QLD 4072, Australia*

² *School of Science, Griffith University, Brisbane QLD 4111, Australia*

Corresponding author e-mail address: sureshb@cheque.uq.edu.au

Introduction

Many of the recently developed applications for microporous materials rely on an accurate understanding of their transport properties, over a range of fluid densities. However, there are significant difficulties in developing a tractable theory that can be used to characterize transport processes in these materials. Indeed, the difficulty in developing an analogous theory to describe transport over a range of fluid densities in macropores has been recognized since the theoretical models of Knudsen [1].

In this paper [2] we consider models for transport in microporous systems. At low densities, where intermolecular interactions are rare, we consider a statistical mechanical transport model. At higher densities, we consider two hydrodynamic slip models. Each of the models presented compares favourably with the computer simulation results for transport of methane in microporous carbon.

Theory

We consider fluid transport along a slit micropore of width H . The micropore is modeled as two infinite walls in the yz plane, with transport along the z axis. The pore-fluid interaction is modeled as a one-dimensional potential $V(x)$ across the pore, and a diffuse boundary condition [3] at the pore wall. In our case, $V(x)$ is defined by choosing the Steele 10-4-3 potential [4] to describe the interaction for each wall. The diffuse condition is described by an accommodation coefficient α , representing the average fraction of a molecule's incident momentum that is lost to the wall during boundary interactions. Intermolecular interactions are modeled using a Lennard-Jones potential.

At low densities, intermolecular interactions are rare, and the dynamics of a molecule is effectively described by the pore-fluid interaction only. For our low-density model, intermolecular interactions serve to 'mix' the energies of the fluid molecules, and are not explicitly included in the calculations of the molecular trajectories. The dynamics are therefore separable, and the quantity $E_x = V(x) + p_x^2/2m$ is a constant of the motion between intermolecular interactions. A molecule oscillates across the pore in a manner

determined by E_x and $V(x)$, and the time τ for a molecule to oscillate across the pore is a function of E_x –

$$\tau(E_x) = \sqrt{2m} \int [E_x - V(x)]^{-1/2} dx, \quad (1)$$

where the integration is performed over the range of x accessible to the molecule. If the system is at thermal equilibrium with its environment, the distribution of states of these oscillating molecules is determined by the canonical (Maxwell-Boltzmann) distribution. From this information, the density and velocity profiles of molecules traveling along the pore can be determined for an external driving force F , from which the flux, and ultimately the transport diffusion coefficient D_0 , can be determined –

$$D_0 = \frac{k_B T}{F} \langle v_z \rangle = \left(\frac{2 - \alpha}{\alpha} \right) \frac{k_B T \int_{-\infty}^{\infty} \int_{-H/2}^{H/2} \tau(E_x(x, p_x)) e^{-E_x(x, p_x) / k_B T} dx dp_x}{2m \int_{-\infty}^{\infty} \int_{-H/2}^{H/2} e^{-E_x(x, p_x) / k_B T} dx dp_x}. \quad (2)$$

We note that it is straightforward to extend the above theory to cylindrical pores [5,6].

As the fluid density increases, the interaction between fluid molecules dominates the solid-fluid interaction, and the oscillator model no longer captures the essential behavior of diffusing molecules. At high densities, therefore, we turn to an alternative model – a slip flow model [7,8]. As with the low-density model, the aim of the model is to develop an expression for the mass flux, from which D_0 can be determined. The density profile is obtained from an appropriate density functional theory, or from molecular simulation. The velocity profile is obtained from the Navier-Stokes relation

$$\frac{d}{dx} \left(\eta(x) \frac{dv_z(x)}{dx} \right) = -F(x) \rho(x), \quad (3)$$

where $\eta(x), v_z(x), \rho(x), F(x)$ represent the viscosity, velocity and density profiles, and the mean external force at x . The viscosity profile can be estimated from an equilibrium density correlation [9], and Eqn.(2) integrated to obtain the velocity profile across the pore. Two boundary conditions are required – a symmetry condition, and a frictional slip condition at the boundary x_0 , of the form

$$mv_z(x_0) Z_0 = -\eta(x) \frac{dv_z(x)}{dx}$$

where Z_0 represents the frequency of reflections at the pore wall, which can be estimated from kinetic theory. The diffusion coefficient for this model (model A) is

$$D_0^A = \frac{2k_B T}{\hat{\rho} H} \left[\frac{1}{m Z_0} \left(\int_{-x_0}^0 \rho(\xi) d\xi \right)^2 + \int_{-x_0}^0 \frac{1}{\eta(\xi)} \left(\int_{\xi}^0 \rho(\zeta) d\zeta \right)^2 d\xi \right], \quad (4)$$

with mean pore density $\hat{\rho}$. The first term in the square brackets represents a boundary contribution; the second term represents a viscous contribution. At low density, as the viscous contribution goes to zero, we expect the boundary term to converge to the oscillator result. As an alternative model (model B), we propose

$$D_0^B = D_0^{OSC} + \frac{2k_B T}{\hat{\rho} H} \int_{-x_0}^0 \frac{1}{\eta(\xi)} \left(\int_{\xi}^0 \rho(\zeta) d\zeta \right)^2 d\xi. \quad (5)$$

Simulation Details

We apply the theory developed above to the transport of methane in microporous carbon, with $H < 2$ nm. The potential in each slit pore is determined using the Steele 10-4-3 potential for each wall, and diffuse boundary conditions were applied ($\alpha = 1$) during molecular dynamics (MD) runs. Grand canonical Monte Carlo (GCMC) simulations were performed to determine density profiles, and generate initial conditions for MD simulations. D_0 was measured from both equilibrium MD (EMD) and nonequilibrium MD (NEMD). For equilibrium simulations, D_0 was determined from the Green-Kubo expression – the autocorrelation function of the center-of-mass velocity:

$$D_0 = \frac{1}{N} \lim_{\tau \rightarrow \infty} \int_0^{\tau} \left\langle \sum_{i,j} v_{zi}(0) v_{zj}(t) \right\rangle dt. \quad (6)$$

For nonequilibrium simulations with external force F , D_0 was determined via the flux J

$$D_0 = J k_B T / \hat{\rho} F. \quad (7)$$

Results and Discussion

The transport coefficients determined from EMD and NEMD were in good agreement with one another (see Figs. 1 and 2), consistent with observations from other studies. At low densities (Henry's Law region), D_0 remains constant. In the 1.0 nm pore, D_0 decreases with increasing density – as the density increases, the rate of diffuse collisions increases, lowering the overall transport rate. In the wider pores, D_0 increases until a local maximum is reached. The viscous forces appear to drive this increase as central layers of fluid molecules form, until the presence of these layers also increases the rate of diffuse collisions.

We observe excellent agreement between the low-density simulation data and the oscillator model, as seen in Figure 3. The model predictions for the transport coefficient, the density profile and the velocity profile are all supported by the simulation results. Furthermore, the oscillator model prediction for D_0 can be applied up to densities of 1 nm^{-3} , corresponding to bulk pressures of one atmosphere.

We note that the significant difference between the two high-density models derives from the boundary term. In model A, it is a functional of the density profile; in model B it is a functional of the fluid-pore interaction potential, and therefore independent of

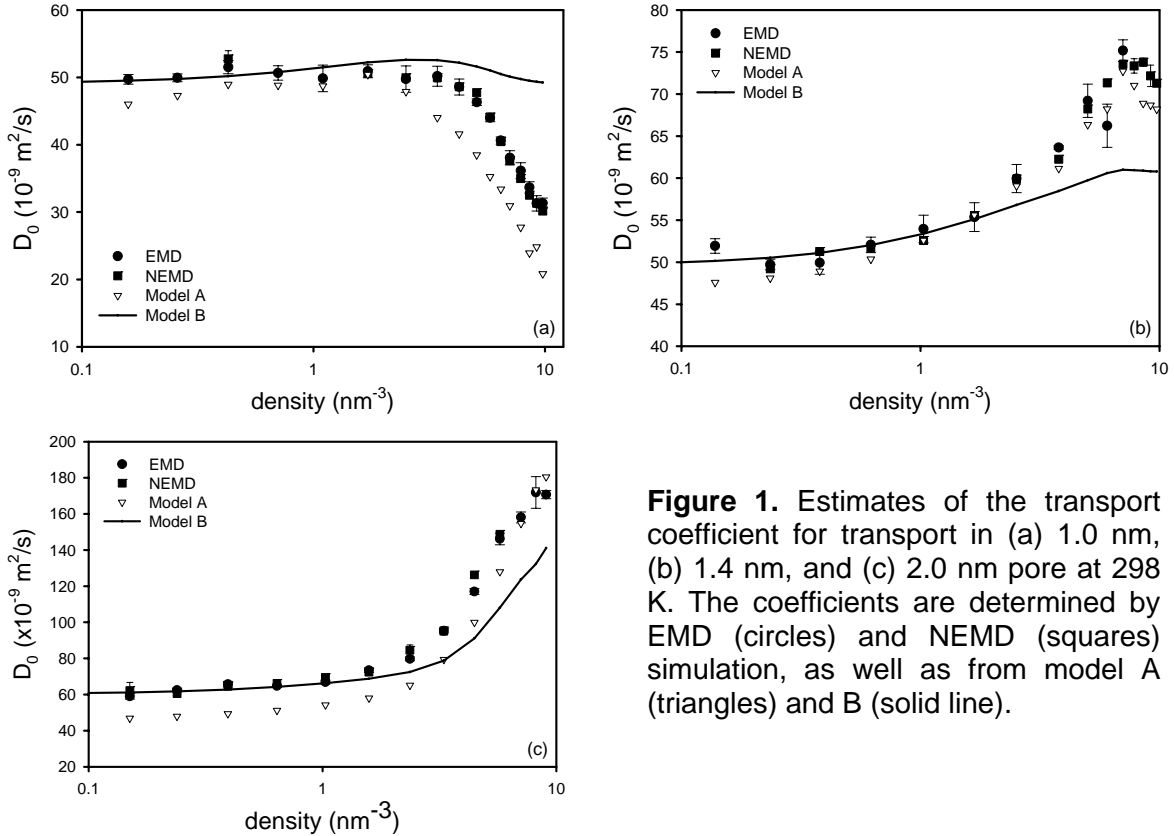


Figure 1. Estimates of the transport coefficient for transport in (a) 1.0 nm, (b) 1.4 nm, and (c) 2.0 nm pore at 298 K. The coefficients are determined by EMD (circles) and NEMD (squares) simulation, as well as from model A (triangles) and B (solid line).

density. We observe from Figs. 1 and 2 that both models agree well with the simulation results of the systems examined, although model B fails at high density in the 1.0 nm pore. This is because the viscous contribution in the model is always positive, but the trend in D_0 is negative. This is consistent with our interpretation of this negative trend in terms of boundary collisions. Overall, model A predicts well in the 1.4 nm pore, underpredicts the density-dependent effects in the narrower pore, and overpredicts these effects in the wider pore. The boundary term of model A appears to become less reliable as the pore width increases. Model B appears generally to overestimate the density effect on the transport coefficient, indicating that some of these effects are compensated by the change in density-dependence of the boundary interaction. We note that model B becomes more reliable as the pore width increases.

Conclusions

In the Henry's Law regime, the dynamics are dominated by the solid-fluid interaction potential, and the oscillator model provides a good estimate for the transport behavior. The oscillator model appears to capture the essential details of low-density transport. At higher densities, we present two hydrodynamic transport models, with boundary conditions determined by a slip condition (model A) or based on the oscillator model (model B). Both model the transport processes as a combination of boundary and viscous effects, and provide valuable insight into the complex interplay between these two effects as the density changes.

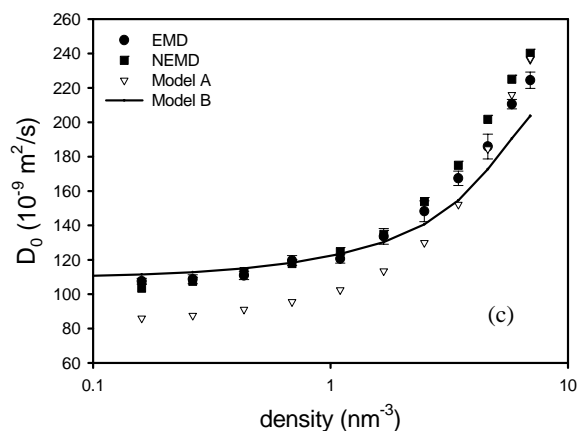
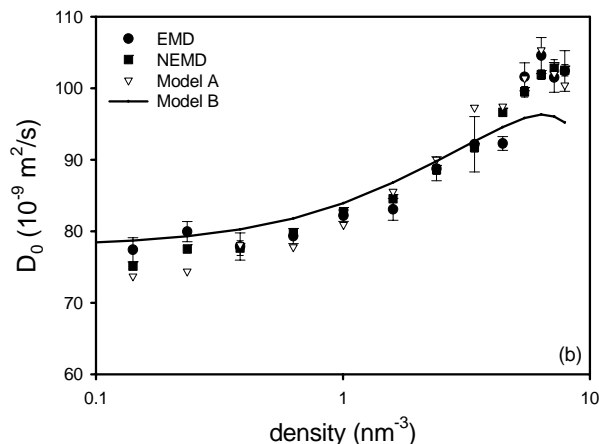
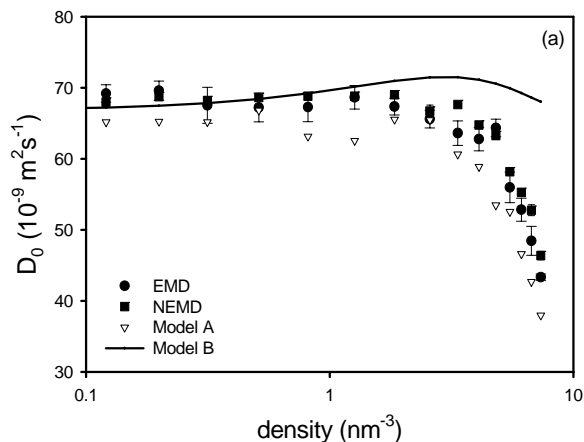


Figure 2. Estimates of the transport coefficient for transport in (a) 1.0 nm, (b) 1.4 nm, and (c) 2.0 nm pore at 400 K. The coefficients are determined by EMD (circles) and NEMD (squares) simulation, as well as from model A (triangles) and B (solid line).

References

- [1] M. Knudsen, *Ann. Physik.* 1909;28:75.
- [2] O. G. Jepps, S. K. Bhatia, and D. J. Searles, *J. Chem. Phys.* 2004; in press.
- [3] R. F. Cracknell, D. Nicholson and N. Quirke, *Phys. Rev. Lett.* 1995; 74:2463.
- [4] W. A. Steele, *The Interaction of Gases with Solid Surfaces*, Oxford: Pergamon, 1974.
- [5] O. G. Jepps, S. K. Bhatia, and D. J. Searles, *Phys. Rev. Lett.* 2003; 91:126102.
- [6] S. K. Bhatia, O. G. Jepps and D. Nicholson, *J. Chem. Phys.* 2004; in press.
- [7] S. K. Bhatia and D. Nicholson, *Phys. Rev. Lett.* 2003; 90:016105.
- [8] S.K. Bhatia and D. Nicholson, *J. Chem. Phys.* 2003;119:1719.
- [9] T.H. Chung, M. Ajlan, L.L. Lee and K.E. Starling, *Ind. Eng. Chem. Res.* 1988; 27: 671.

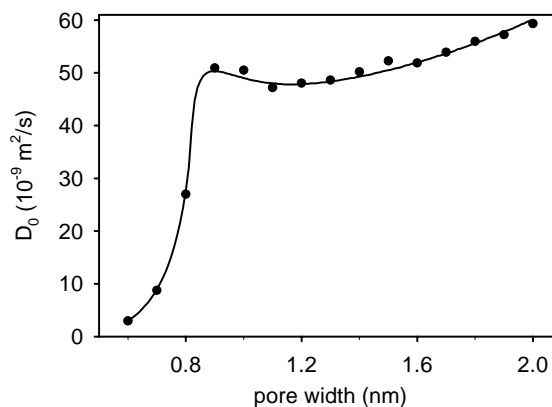


Figure 3. Low density model: Variation of transport coefficient with slit width for the adsorption of methane at 298 K in carbon slit pores. The line corresponds to the model predictions and symbols to simulation data.